

## Bilayers of Nucleosome Core Particles

Amélie Leforestier,\* Jacques Dubochet,<sup>†</sup> and Françoise Livolant\*

\*Laboratoire de Physique des Solides, Bât 510, Université Paris Sud, F-91405 Orsay Cedex, France and <sup>†</sup>Laboratoire d'Analyse Ultrastructurale, Bât de Biologie, Université de Lausanne, CH-1015 Lausanne, Switzerland

**ABSTRACT** Among the multiple effects involved in chromatin condensation and decondensation processes, interactions between nucleosome core particles are suspected to play a crucial role. We analyze them in the absence of linker DNA and added proteins, after the self-assembly of isolated nucleosome core particles under controlled ionic conditions. We describe an original lamellar mesophase forming tubules on the mesoscopic scale. High resolution imaging of cryosections of vitrified samples reveals how nucleosome core particles stack on top of one another into columns which themselves align to form bilayers that repel one another through a solvent layer. We deduce from this structural organization how the particles interact through attractive interactions between top and bottom faces and lateral polar interactions that originate in the heterogeneous charge distribution at the surface of the particle. These interactions, at work under conditions comparable with those found in the living cell, should be of importance in the mechanisms governing chromatin compaction *in vivo*.

### INTRODUCTION

Despite uncertainties in the conformation of the histone *N*-termini, the structure of the nucleosome core particle is now solved at atomic resolution (Lüger et al., 1997; Harp et al., 2000), and the challenge is to understand the higher orders of chromatin organization. In the living cell, chromatin remains condensed throughout the cell cycle, but dynamical changes of its level of folding must occur to allow portions of the genome to be transcribed or replicated at a given time, resulting in local DNA concentration fluctuating between 50 and 250 mg/ml. Although there is now accumulation of evidence that higher order structures play a key role in the regulation of gene expression (Van Holde, 1988; Orphanides and Reinberg, 2000; Strahl and Allis, 2000), little is known about the interactions that maintain and stabilize the multiple and flexible compacted forms of chromatin, and how they are modified during the cell cycle.

*In vitro*, isolated chromatin fibers can also compact or extend, in high and low ionic strength, respectively (Fletcher and Hansen, 1996; Widom, 1986, 1998). Multiple components are involved in the condensation process, and the fiber conformation appears as the result of a complex interplay of many factors, including the ionic environment, binding of linker histones, terminal extensions of the core histones, and linker DNA length, which specific roles remain difficult to assign and characterize (Van Holde and Zlatanova, 1996). We address here a simpler but fundamental question: how do the building blocks of the chromatin fiber, the nucleosome core particles (NCP), interact in the range of concentration of the cell?

To approach the question, we investigate the self-assembly of isolated NCP under controlled ionic environment.

The richness of the phase diagram extending from irregular piles of particles, through various liquid crystalline phases (Leforestier and Livolant, 1997; Leforestier et al., 1999; Livolant and Leforestier, 2000) to three-dimensional crystals (Lüger et al., 1997; Dubochet and Noll, 1978; Finch and Klug, 1978), demonstrates that there is a lot to learn from this approach. In this work, we report the formation of a novel lamellar mesophase which is described at length scales ranging from micrometers to nanometers using optical microscopy and cryoelectron microscopy of ultrathin sections of vitrified solutions. This analysis provides unique and direct insights into the intermolecular contacts, and allows to deduce how the molecules interact and organize under well defined and controlled conditions.

### MATERIALS AND METHODS

#### Materials

Nucleosome core particles ( $145 \pm 3$  base pairs (bp) DNA) and H1-depleted nucleosomes ( $167 \pm 10$  bp) were respectively prepared from native chicken erythrocyte and calf thymus chromatin as described previously (Leforestier and Livolant, 1997). Both were checked to contain all four intact histones. After purification by gel chromatography (Sephacryl S300, Pharmacia, Uppsala, Sweden), the solutions were extensively dialyzed against 5 mM NaCl, 10 mM Tris, and 1 mM EDTA (pH 7.6). They were concentrated up to 250 mg/ml by ultrafiltration in a pressurized cell (Amicon 8010, Amicon Corp., Lexington, MA). Higher concentrations were reached by increase of the osmotic pressure, imposed by a neutral stressing polymer (polyethylene glycol, Fluka MW 20000, Fluka Chemical Corp., Milwaukee, WI). The solutions were equilibrated against the polymer dissolved in the same buffer at 19, 20, or 22% (w:w) after two different procedures: (1) extensive dialysis (3 weeks) through a cellulose membrane; or (2) progressive mixing of the nucleosome and polymer solutions by successive introduction of given volumes of the two solutions into flat glass capillaries (Vitro Dynamics, Rockaway, NJ), and subsequent equilibration for weeks. Both procedures yield equilibrium samples and result in the same structures. The illustrations presented here are recorded from samples obtained with H1-depleted nucleosomes (167 bp) by procedure 1 (Fig. 1, *b–d*) or 2 (Fig. 1 *a*, Fig. 2). Similar data were recorded with nucleosome core particles (146 bp).

Received for publication 21 March 2001 and in final form 22 June 2001.

Address reprint requests to Françoise Livolant, Laboratoire de Physique des Solides, Bât 510, Université Paris Sud, F-91405 Orsay Cedex, France. Tel.: 33-1-60-15-53-92; Fax: 33-1-69-15-60-86; E-mail: livolant@lps.u-psud.fr.

© 2001 by the Biophysical Society

0006-3495/01/10/2414/08 \$2.00

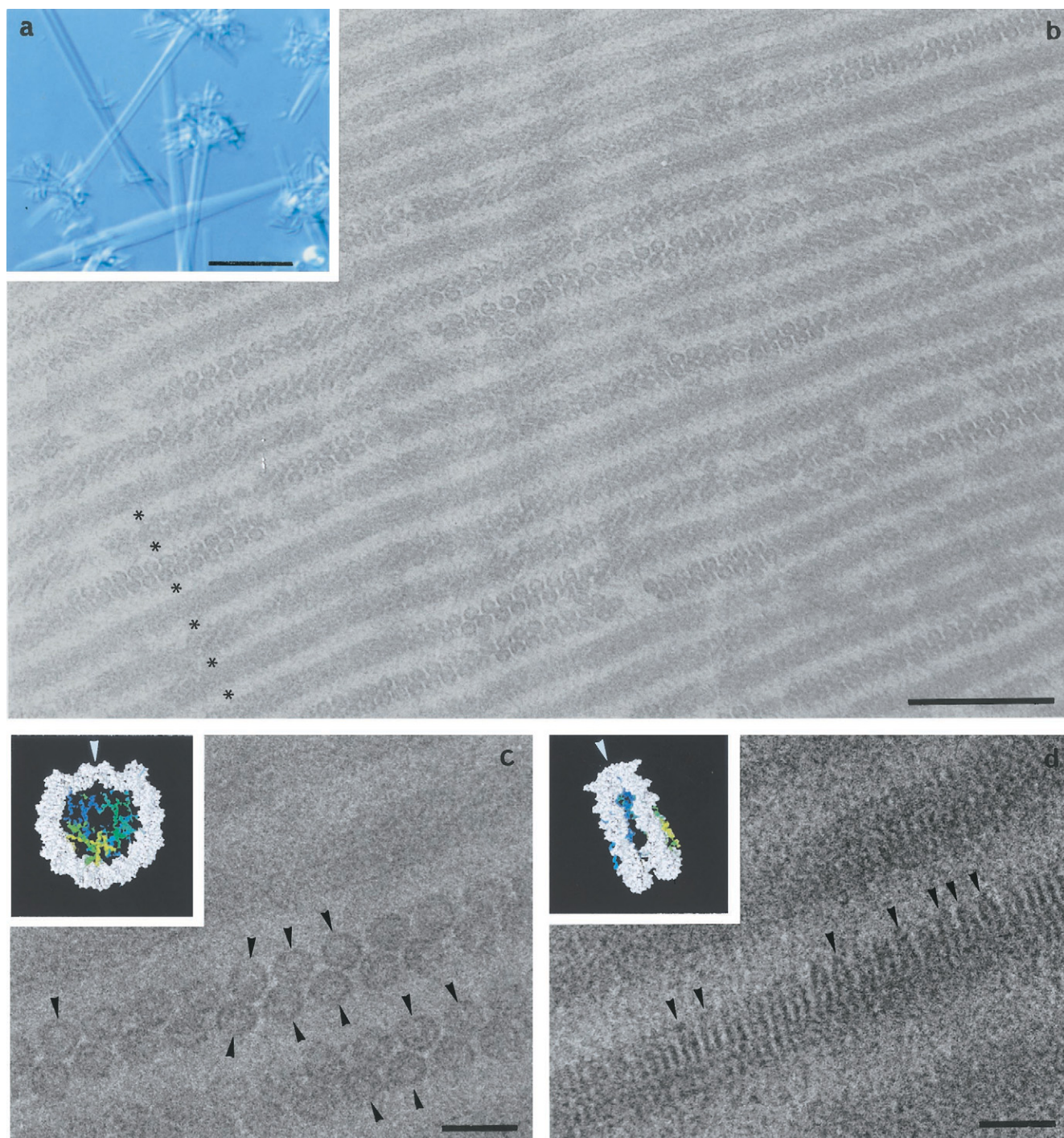


FIGURE 1 Structure of the lamellar phase. (a) Tubules observed in light microscopy (Nomarski interferential contrast). (b–d) The lamellar structure is revealed by cryoelectron microscopy of vitreous sections. Bilayers of columns of NCP interspaced with solvent layers (\*) are observed in cross-section. The bilayer structure is best visualized when the columns are oriented perpendicular (some regions of *b* and *c*) or parallel (*d*) to the observation plane. In top view (*c*), NCPs appear as disc-like objects delineated by the well contrasted DNA peripheral crown. The protein core of the particle is not homogeneous. Its low density area can be related to the particle's inner structure (*inset*; from PDB 1aoi, (Lüger et al., 1997), and allows orientation of the dyad axis  $\delta$  (*arrowheads*). In side view (*d*), NCP are visualized as well, contrasted stripes corresponding to the gyres of the DNA molecule around the particle. When  $\delta$  lies perfectly parallel to the observation plane (*arrowheads*), the NCP seem V-shaped with the tip of the V pointing to the solvent layer. Note that, on this micrograph, this striation is clearly visible along one half of the bilayer only (whereas the facing layer of the lamella seems fuzzy). Scale bars: 20  $\mu\text{m}$  (*a*); 100 nm (*b*); 20 nm (*c*, *d*).



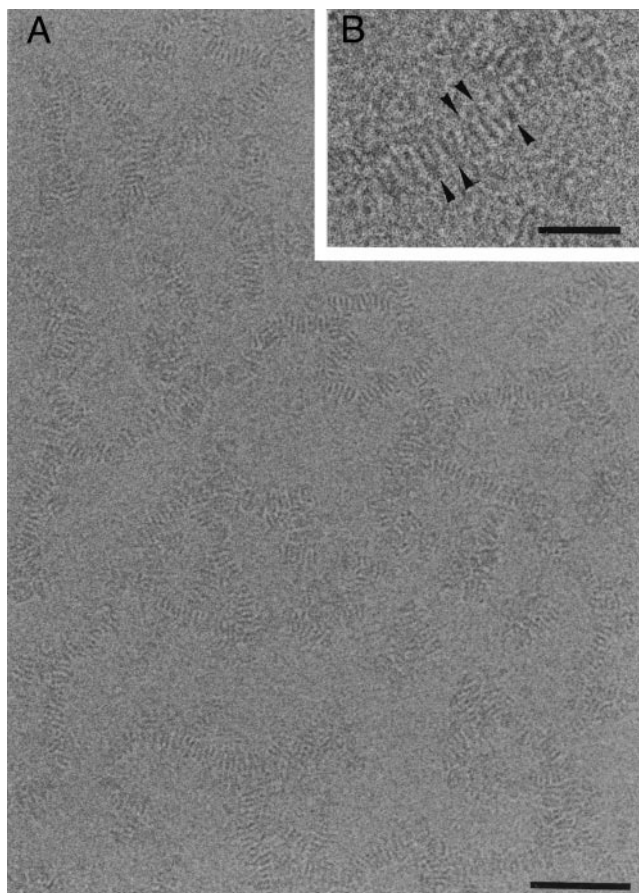


FIGURE 2 Isotropic solution with columns forming a branched random network (*a*). All orientations of the dyad axis are observed along a given column, indicating that the particles are free to rotate around their superhelical axes. Among these, V patterns observed when  $\delta$  lies in the plane are pointed out (arrowheads), showing that particles can stack parallel (VV) as well as antiparallel (AV) (*b*). All intermediates are also found. Scale bars: 50 nm (*a*) and 20 nm (*b*).

### Optical microscopy

Glass capillaries were observed in a Nikon Optiphot X Pol microscope (Nikon Corp., Tokyo, Japan) equipped with an interferential Nomarski contrast device.

### Cryoelectron microscopy

To investigate the bulk structure of the lamellar phase, drops of the solution were vitrified by projection against a copper surface cooled down to 10 K with liquid helium (Cryovacublock, Leica-Reichert, Vienna, Austria). Ultrathin cryosections were realized at 113 K under nitrogen atmosphere in a cryomicrotome (Leica, Vienna, Austria), following the method described in (Sartori and Salamin, 1998). The thin-film vitrification technique (Dubochet et al., 1988) was used to investigate concentrated isotropic solutions: drops were deposited onto a platinum-carbon film with holes and blotted with filter paper; the remaining thin film spanning the holes was immediately vitrified by immersion in liquid ethane. To minimize water evaporation (Cyrklaff et al., 1990), the procedure was performed under a humidified atmosphere.

Sections and thin films were observed at 100 K in a Philips CM 12 cryo-TEM (Philips, Dulphe, Netherlands) at 80 kV. The vitreous state of

the water was checked by electron diffraction, and images were recorded in low-dose mode at a direct magnification of 45,000 $\times$  at 800–900 nm under-focus. The thickness of the sections, calculated by optical density measurements on negative films (Chang et al., 1983), varies from 50 to 80 nm.

## RESULTS

We investigated the self-assembly of two types of macromolecular complexes: nucleosome core particles, with 146 bp DNA associated to the octamer core; and H1-depleted nucleosomes, with 167 bp DNA. We have found no difference in their supramolecular organization, from the micrometer scale to the nanometer scale. Both will be hereafter referred to as NCP.

A mesophase, specific of “low added salt conditions,” forms in the range of 300 to 370 mg/ml NCP in solutions dialyzed against 3.5 to 35 mM monovalent salt (NaCl + Tris-Cl). These concentrated solutions exhibit tubular textures in optical microscopy (Fig. 1 *a*). Isolated tubules are typically 1 to 10  $\mu$ m in diameter and 10 to 200  $\mu$ m long. They may also be connected to one another and even form dense spherulites.

Cryoelectron microscopy of ultrathin sections of vitrified samples reveals that the tubule walls correspond to a lamellar structure, observed in cross-section in Fig. 1 *b*. Each lamella is formed by a bilayer of parallel columns of NCP, clearly visible when the columns are oriented along the observation direction (some regions of Fig. 1, *b* and *c*). These bilayers (17–19 nm thick), alternate with layers of solvent to form a long range lamellar structure which period  $P$  may vary from 27 to 42 nm. The thickness of the solvent layer varies from 9 to 22 nm depending on the NCP concentration. Fluctuations are also observed in the arrangement of NCP columns within the bilayers. Distances between columns ranges from 8.6 to 12 nm. The center to center distance between adjacent columns on a given side of the bilayer ( $a_2$ ) may be either larger or smaller than the distance separating adjacent columns from opposite sides ( $a_1$ ). On Fig. 1 and related micrographs taken from the same sample, the distances  $a_2$  and  $a_1$  are respectively equal to  $10.9 \pm 0.2$  nm and  $12 \pm 0.2$ . Moreover, in columns seen down their axis, projections of the nucleosome core particles may be circular or slightly elliptical (Fig. 1 *c*), indicating a possibility for the NCP to tilt inside the columns. We suspect that these fluctuations may originate from local distortions of the layering. Columns parallel to the section plane stand at another favorable view, showing the particles piled on top of one another with a stacking distance of 5.9 to 6.9 nm (Fig. 1 *d*). These data are in agreement with x-ray diffraction experiments performed in parallel at room temperature (S. Mangenot, D. Durand, A. Leforestier, F. Livolant, in preparation).

The orientation of the columns may vary slightly inside a given bilayer; it can change abruptly between successive layers. The lamellar structure also presents numerous de-

fects and distortions, such as discontinuous bilayers, dislocations, curvature of the lamellae, etc., which will be analyzed in detail elsewhere.

The polarity of the NCP orientation within the bilayers is readily visible on the micrographs. When columns are seen in top view (Fig. 1 *c*), DNA at the periphery seems darker than the protein core and underlies the outskirts of the particle. A portion of the DNA crown, located on the outer side of the bilayer, may look less marked. The protein core itself shows an heterogeneous density distribution, with a region of lower density facing the outer side of the bilayer. Comparison of the micrographs with the crystallographic model of Luger et al. (1997) (Fig. 1, insets) allows orientation of the dyad axis  $\delta$  (arrowheads): NCP are positioned back to back in the bilayer and their front sides, with the free DNA ends, facing the solvent layer. This is confirmed when the columns are oriented parallel to the section plane (Fig. 1 *d*). NCP are seen in side view, and DNA draws a typical V-shape pattern, with the V pointing toward the solvent layer. However, the micrographs demonstrate that the orientation of the particles is not strictly defined: perfect V-patterns are not always observed, revealing slight rotations around the column's axis. This variability is also observable in top view projection, from the irregular orientation distribution of the lower density region of the histone core (Fig. 1, *b* and *c*). The analysis of this distribution shows that the orientation of the dyad axis  $\delta$  is on average normal to the bilayer, but fluctuates by  $\pm 35^\circ$  around this average. When columns are seen in top view, the number of NCP within the thickness of the section varies from 7–9 (for a section 50 nm thick) to 11–13 (for a section 80 nm). Only 4–6 NCP are superimposed in side views. On account of the rotational degree of disorder of NCP observed in top and side views, we must exclude the possibility that NCP could be in perfect rotational register throughout the thickness of the section. The imaging of the particles' fine details, as observed in Fig. 1, *c* and *d*, suggests that, although all NCP should contribute to the image formation, high-resolution detail comes from a single particle. We may hypothesize that other contributions cancel one another to form the background signal. Understanding the image formation in crowded samples is a challenging and crucial question in cryoelectron microscopy. This material may be specially suited to address this question, although preliminary sets of tilt experiments did not provide definitive answers. A more detailed analysis is being undertaken to understand the images.

This remarkable bilayer structure prompted us to search for preceding steps of organization in a lower range of NCP concentration. Isolated columns of nucleosome core particles were found under identical ionic conditions in a small range of NCP concentration between 250 and 300 mg/ml. They were observed by cryoelectron microscopy of vitrified thin films (Fig. 2) performed under a humid atmosphere. In some preparations, these columns were observed in coexistence with isolated bilayers, trapped in the liquid film.

Such biphasic samples attest that the ionic conditions of the film were not significantly changed before freezing because the lamellar structure disappears when the salt concentration is increased  $>0.35$  M. The presence of these columns was also confirmed by independent observations in optical microscopy: the isotropic solution, extinguished between crossed polars, becomes illuminated under shear. This flow-induced birefringence reveals that NCP are not isolated, but self-associated into larger aggregates such as these columns. Semiflexible columns, made of  $\sim 5$ –25 particles, are oriented in the plane of the film, and connected into an isotropic network. The interesting point is that, in these columns, NCP stack without apparent rotational constraint. Contrary to the lamellar liquid crystal, there is no orientational order of the particles along the columns: all possible side view projection patterns of the particle are found randomly dispersed along the column.

## DISCUSSION

Over a defined range of monovalent salt concentration (3.5–35 mM), isolated nucleosome core particles self-assemble to form a lamellar phase which periodicity varies from  $\sim 27$  to 42  $\mu\text{m}$ . This variation comes mainly from changes in the thickness of the solvent layer (to accommodate different amounts of solvent) because the phase is observed over a range of NCP concentration comprised between  $\sim 300$ –370 mg/ml. We do not consider here the geometrical problems arising from the chiral structure of the nucleosome core particles which are probably responsible for the coiling of the layers, thus forming these tubular structures seen on Fig. 1. We focused our attention on the formation of the bilayers whose stability depends on ionic conditions. Indeed, for monovalent salt concentrations  $>35$  mM, the lamellar phase disappears. Two-dimensional or three-dimensional ordered hexagonal phases are observed instead (Leforestier and Livolant, 1997; Livolant and Leforestier, 2000, and unpublished data). Fig. 3 summarizes the two steps leading to the formation of the lamellar phase with the increase of particle concentration: the primary association of nucleosome core particles into columns via top to bottom interactions; and the parallel alignment of the columns into bilayers, coupled to a reorientation of NCP.

The formation of columns of isolated NCP is a general feature, previously reported many times. Under crystallization conditions, isolated columns were observed in classical transmission electron microscopy before visible crystals appeared or in coexistence with the crystals. The relative orientation of stacked particles is strictly defined and leads either to linear, wavy, arched, or helical columns because of the wedge shape of the cylinder (Dubochet and Noll, 1978; Finch and Klug, 1978; Finch et al., 1981; Struck et al., 1992). Isolated columns resulted also from the aggregation of NCP induced by addition of divalent or trivalent cations to a dilute solution of NCP (Grau et al., 1982; Leforestier et

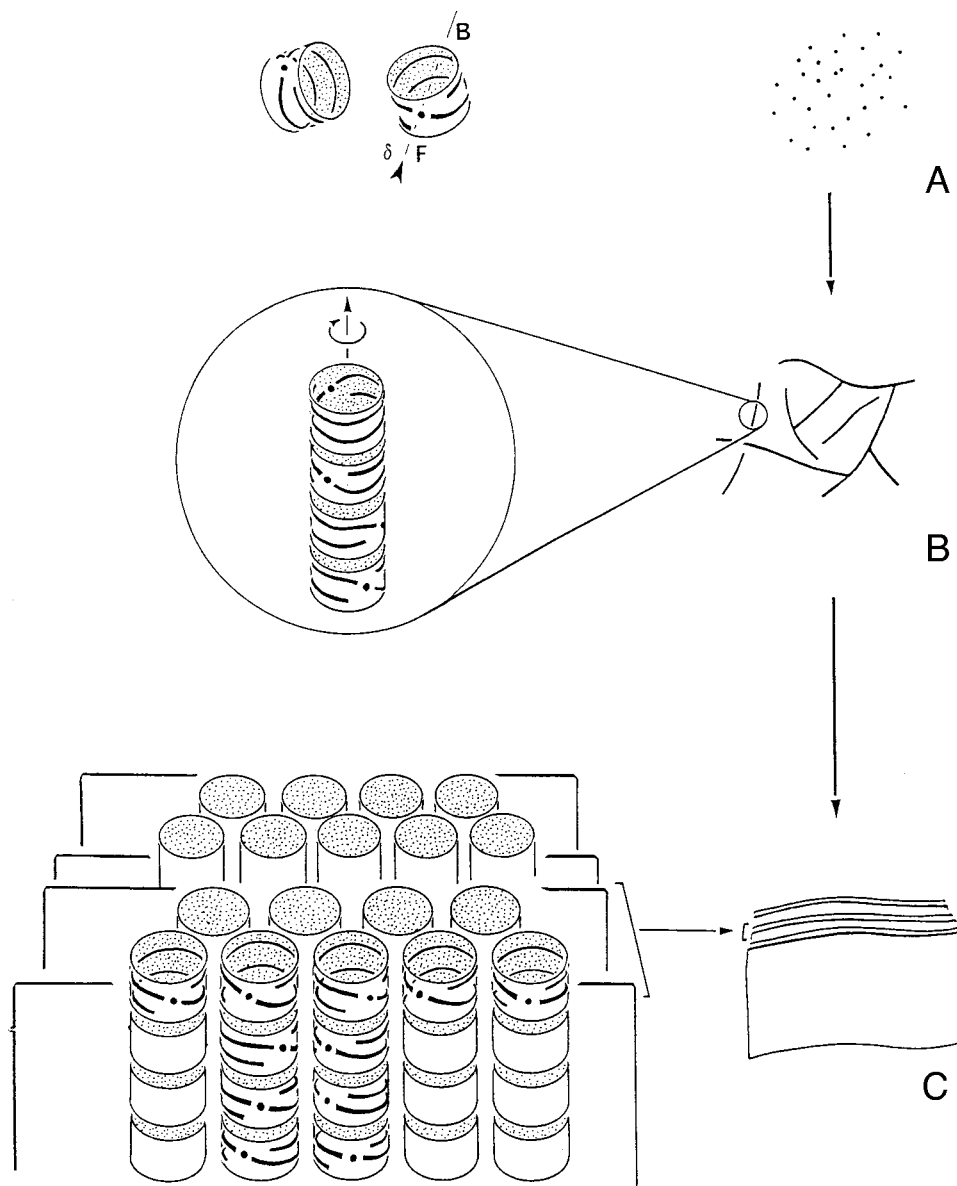


FIGURE 3 Evolution of the supramolecular organization, from isotropic (*a*) to columnar isotropic (*b*) and lamellar (*c*). (*a*) The entry (arrowhead) and exit sites of the dyad axis ( $\delta$ ), determine the front (*F*) and back (*B*) sides of the NCP. (*b*) Above a threshold concentration, NCP pile on top of one another to form columns. All possible orientations of  $\delta$  are allowed and the column as a whole possesses a rotational symmetry. (*c*) Bilayers are formed by the parallel alignment of the columns. In each of them, NCP reorient with their *F* sides facing the solvent layer, although keeping some slight rotational freedom. NCP may be tilted in the columns, but for convenience, they are drawn here all perpendicular to the main axis of the columns.

al., 1999). In the presence of the trivalent spermine, we previously showed that NCP stack on top of one another with no preferential relative orientation and at stacking distances slightly higher than those of crystalline columns. We report here that isolated columns of NCP also form in the absence of any aggregation agent but at high NCP concentration. Such columns, formed by randomly stacked NCP, form over a very wide range of  $\text{Na}^+$  concentration (from a few mM to  $>150$  mM  $\text{Na}^+$ , data not shown).

Forces involved in the stabilization of NCP columns may therefore be of two types. First are nonspecific attractive

interactions between top and bottom faces of the particles that allow the particles to rotate freely through the solvent. These interactions are not dominated by electrostatics because columns remain present under highly diverse ionic conditions (altogether in concentration and valency). [Note that because we cannot distinguish the top and bottom faces of the particles, we cannot preclude the occurrence of top/top and bottom/bottom interactions.] Second, more specific interactions may further stabilize one or a few defined relative orientations. The precise particle positioning in crystalline columns, for example, apparently involves elec-

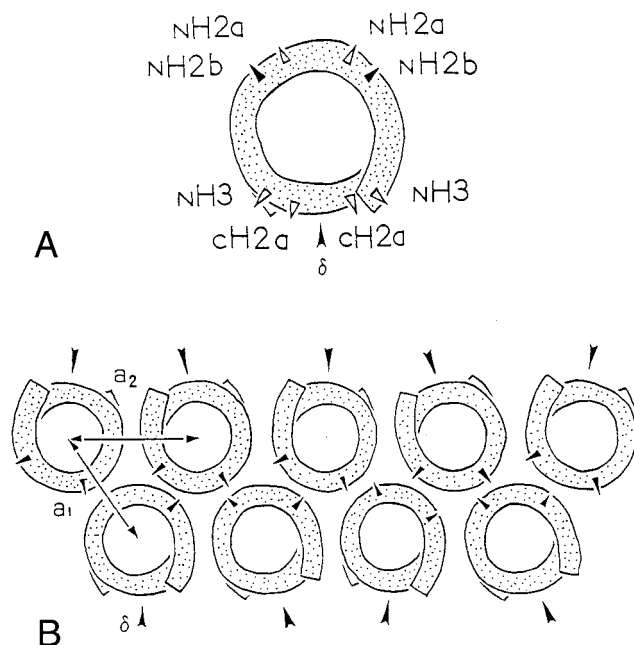


FIGURE 4 Top view of the NCP orientation in the bilayer structure. Exit sites of the histone tails, indicated by *arrowheads* in (a), show that NH2b (and possibly NH2a) tails are most likely involved in the stabilization of the bilayer, because of their position on the back side of the NCP.

trostatic contacts established through histone tails, between the basic *N*-terminal domain of histone H4 and 7 clustered acidic side chains of the H2a-H2b dimer (Lüger et al., 1997; Finch and Klug, 1978).

At least two types of interactions are necessary to stabilize the bilayered lamellar phase: one to maintain columns in the bilayer, and the other to stabilize the bilayers at a given distance one from the other. These interactions between lateral faces of the nucleosomes are strongly dominated by electrostatics. Indeed, columns lose their polarity when the lamellar phase disappears as the NaCl concentration is raised (in preparation). Considering the structure of the nucleosome core particle and the geometry of the bilayer (Fig. 3, c; Fig. 4), we suspect that these interactions originate from the heterogeneous charge distribution on the lateral surface of the particles: negative phosphate charges on DNA strands and positive charges on the basic terminal extremities of the histones extruding laterally, N-H2b and N-H2a on the back side, N-H3 and C-H2a on the front side. We can rule out a crucial role of the linker DNA in this arrangement, as the lamellar phase remains unchanged whatever the length of DNA associated to the histone core (146 or 167 bp). The highly charged NH2b tails protruding at 35° on both sides of the dyad axis are most likely responsible for the bilayer structure. They would make adjacent NCP come into semiclose contact, either through attractive interactions between their positive charges and the DNA negative charges, or by simply screening the repul-

sions between the DNA phosphates of adjacent NCP in this direction. Pointing out of the bilayer, the long N-H3 tails as well as the C-H2a, also highly positively charged, apparently do not interact laterally with adjacent NCPs; indeed, the distance separating surfaces of neighboring particles from a given side of the bilayer is slightly larger than the distance between particles from both sides. The distance between bilayers could be far apart because of electrostatic repulsions between front sides of the particles. However, the thickness of the solvent layer (up to 23 nm), exceeds the Debye length ranges (2–5 nm under our ionic conditions). Long-range interactions have to be considered here, although these interactions are left to nature to be determined.

Based on the experimental work of Widom (1986), Clark and Kimura (1990) concluded from their theoretical approach that the mechanism of chromatin-folding *in vitro* is essentially governed by repulsions between linker DNA segments, and adequately described by Manning's polyelectrolyte theory (Manning, 1978). Nevertheless, the presence of nucleosome-nucleosome interactions is often implicitly assumed (Van Holde and Zlatanova, 1996; Yao et al., 1991; Cui and Bustamante, 2000), and we present here new arguments for their occurrence. We show that the continuity of the DNA molecule is not required to form nucleosome fibers, nor the presence of H1/H5 histones as already reported (Grau et al., 1982; Leforestier et al., 1999). The attractive interactions at work between top and bottom faces of the isolated NCP are more likely arising from the histone cores themselves, which may also form fibers on their own (Sperling and Wachtel, 1981). We may wonder whether, in chromatin, this stacking into columns could be impeded by the continuity of the DNA molecules and/or the presence of the additional negatives charges of the linker DNA, which, in a first approximation, could be expected to lower or counterbalance the top/bottom attractive interactions. From a geometrical point of view, both the distance and the relative orientations of stacked NCP fluctuate along the columns, which should make it possible to suit the presence of the linker DNA. Also, *in vitro* experiments performed by Tatchell and Van Holde (1978) have shown that these interactions may induce a sliding of the core histones along the DNA. We may therefore imagine that successive particles along the DNA chain could well stack on top of one another into 11-nm fibers. This hypothesis is supported by the observation of a 11-nm optical diffraction ring in cryosections of vitrified metaphase chromosomes (McDowall et al., 1986).

Our experiments also revealed that lateral interactions between NCP are strong enough to produce a rotation of the NCP around their axis while they are already stacked into columns, and suggest that the H2b (and eventually H2a) histone tails play a crucial role, stabilizing back-to-back interactions (and perhaps being responsible for the close approach of the particles). These interactions cannot come into play in isolated chromatin fibers, which explains why



H2a/H2b tails were found to contribute only marginally to the cation-induced folding of nucleosomal arrays (Moore and Ausio, 1997; Tse and Hansen, 1997; Widom, 1998). However, in the cellular context, in which nucleosomes necessarily come into lateral close contact because of the high macromolecular concentration, these interactions are likely to play an essential role in the higher order of chromatin organization.

The next question is whether such a lamellar liquid crystalline structure may represent a possible model for chromatin organization in vivo. A major requirement has been met: the DNA concentration in the lamellar phase, from 300 to 370 mg/ml (i.e., 150–185 mg/ml DNA), falls in the range of values reported for metaphase chromosomes from different organisms (160–200 mg/ml), whereas close packing of most models of the 30-nm chromatin fiber does not allow reaching such high concentrations (Daban, 2000). Let us now consider how the introduction of a linker DNA between the particles could influence their liquid crystalline ordering. From an electrostatic point of view, we have found that the length of the DNA fragments associated with the particles is not a crucial parameter, in the range 146–167 bp. Although we did not check how much a larger DNA/histone ratio would modify the particles' interactions, it can be expected merely to shift the phase boundaries (because of the increase of negative charges). Geometrically, the continuity of the DNA does not preclude such a structure. In the lamellar phase, the entry and exit sites of the DNA on the protein core are facing the solvent layer, so that linker DNA could join the particles, either along the columns with successive NCP stacked on top of one another or across the solvent layer. There is no evidence of such a lamellar structure in classical eukaryote nuclei, but in situ data are so sparse that we cannot ascertain that it does not exist, especially in an out-of-equilibrium system such as the active nuclei where any (liquid crystalline) ordering is expected only transiently and locally. Long-range organizations could be found only in special situations. Interestingly, a lamellar structure (with a period in the range of 50 nm) was described in certain states of the spermiogenesis of the fish *Scyliorhinus caniculus* by classical transmission electron microscopy (Gusse and Chevaillier, 1978), but further characterization of this chromatin would be necessary to go deeper in the comparison.

To conclude, we propose an original approach to investigate interactions between chromatin components over large ranges of well defined ionic environments. This approach shows how the anisotropic charge distribution of the core particle participates to the establishment of higher order structures. It also allows to propose a more precise scenery of histone tail participation in chromatin organization: under given ionic conditions, N-H2b would stabilize polar lateral interactions between NCP; N-H3 and C-H2a, apparently not involved in lateral nucleosome/nucleosome interactions, would thus be free to stabilize the second turn

of the DNA helix on the protein core or to interact with the linker DNA, in agreement with bibliographical data (Wolffe and Hayes, 1999; Widom, 1998); and N-H4 could stabilize specific top/bottom contacts between NCP (Lüger et al., 1997). By deleting specific tails, or extending this system as to introduce other components involved in chromatin condensation or remodeling (H1 histones, enzymes, linker DNA connecting the nucleosomes, etc.), we may expect further insights in the structures and mechanisms contributing to chromatin function.

We thank N. Sartori-Blanc for counsels and support in the realization of the cryosections. We also thank D. Durand and W. Gelbart for critical reading of the manuscript. We greatly acknowledge the EMBO for supporting A.L. with a short-term fellowship.

## REFERENCES

- Chang, J. J., A. W. McDowall, J. Lepault, R. Freeman, and C. A. Walter. 1983. Freezing, sectioning and observation artefacts of frozen hydrated sections for electron microscopy. *J. Microsc.* 132:109–123.
- Clark, D. J., and T. Kimura. 1990. Electrostatic mechanism of chromatin folding. *J. Mol. Biol.* 211:883–896.
- Cui, Y., and C. Bustamante. 2000. Pulling a single chromatin fiber reveals the forces that maintain its higher-order structure. *Proc. Natl. Acad. Sci. U.S.A.* 97:127–132.
- Cyrklaff, M., M. Adrian, and J. Dubochet. 1990. Evaporation during preparation of unsupported thin vitrified aqueous layers for cryo-electron microscopy. *J. Electron. Microsc. Tech.* 16:351–355.
- Daban, J. R. 2000. Physical constraints in the condensation of Eukaryotic chromosomes. Local concentration of DNA versus linear packing ratio in higher order chromatin structures. *Biochemistry*. 36:11381–11388.
- Dubochet, J., M. Adrian, J. J. Chang, J. C. Homo, J. Lepault, A. W. McDowall, and P. Schultz. 1988. Cryo-electron microscopy of vitrified specimens. *Q. Rev. Biophys.* 21:129–228.
- Dubochet, J., and M. Noll. 1978. Nucleosome arcs and helices. *Science*. 202:280–286.
- Finch, J. T., and A. Klug. 1977. X-ray and electron microscope analyses of crystals of nucleosome cores. *Cold Spring Harb. Symp. Quant. Biol.* 42:1–9.
- Finch, J. T., R. S. Brown, D. Rhodes, T. J. Richmond, B. Rushton, L. C. Lutter, and A. Klug. 1981. X-ray diffraction study of a new crystal form of the nucleosome core showing higher resolution. *J. Mol. Biol.* 145:757–769.
- Fletcher, T. M., and J. C. Hansen. 1996. The nucleosomal array: structure/function relationship. *Crit. Rev. Eukaryotic Gene Express.* 6:149–188.
- Garcia-Ramirez, M., C. Rocchini, and J. Ausio. 1995. Modulation of chromatin folding by histone acetylation. *J. Biol. Chem.* 270:17923–17928.
- Grau, L. P., F. Azorin, and J. A. Subirana. 1982. Aggregation of mono- and dinucleosomes into chromatin-like fibers. *Chromosoma*. 87:437–445.
- Gusse, M., and P. Chevaillier. 1978. Étude ultrastructurale et chimique de la chromatine au cours de la spermiogenèse de la roussette *Scyliorhinus caniculus* (L.). *Cytobiologie*. 16:421–443.
- Harp, J. M., B. L. Hanseine, D. E. Timm, and G. J. Bunick. 2000. Asymmetries in the nucleosome core particle at 2.5 Å resolution. *Acta Crystallographica D*. 56:1513–1534.
- Leforestier, A., S. Fudaley, and F. Livolant. 1999. Spermidine-induced aggregation of nucleosome core particles: evidence for multiple liquid crystalline phases. *J. Mol. Biol.* 290:481–494.
- Leforestier, A., and F. Livolant. 1997. Liquid crystalline ordering of nucleosome core particles under macromolecular crowding conditions:

- evidence for a discotic columnar hexagonal phase *Biophys. J.* 73: 1771–1776.
- Livolant, F., and A. Leforestier. 2000. Chiral discotic columnar germs of nucleosome core particles. *Biophys. J.* 78:2716–2729.
- Lüger, K., A. W. Mäder, R. K. Richmond, D. F. Sargent, and T. J. Richmond. 1997. Crystal structure of the nucleosome core particle at 2.8 Å resolution. *Nature*. 389:251–260.
- Manning, G. S. 1978. The molecular theory of polyelectrolyte solutions with applications to the electrostatic properties of polynucleotides. *Q. Rev. Biophys.* 11:179–246.
- McDowall, A. W., J. M. Smith, and J. Dubochet. 1986. Cryo-electron microscopy of vitrified chromosomes in situ. *EMBO J.* 5:1395–1402.
- Moore, S. C., and J. Ausio. 1997. Major role of the histones H3–H4 in the folding of the chromatin fiber. *J. Biochem. Biophys. Res. Comm.* 230: 136–139.
- Orphanides, G., and D. Reinberg. 2000. RNA polymerase II elongation through chromatin. *Nature*. 407:471–475.
- Sartori, N., and L. Salamin. 1998. Cryo-transmission electron microscopy of thin vitrified sections. In *Cell Biology: A Laboratory Handbook*. E. Celis, editor. Academic Press, Inc., London. 177–185.
- Sperling, R., and E. J. Wachtel. 1981. The histones. *Adv. Protein Chem.* 34:1–60.
- Strahl, B. D., and C. D. Allis. 2000. The language of covalent histone modifications. *Nature*. 403:41–45.
- Struck, M. M., A. Klug, and T. J. Richmond. 1992. Comparison of X-ray structures of the nucleosome core particle in two different hydration states. *J. Mol. Biol.* 224:253–264.
- Tatchell, K., and K. E. Van Holde. 1978. Compact oligomers and nucleosome phasing. *Proc. Natl. Acad. Sci. U.S.A.* 75:3583–3587.
- Tse, C., and J. C. Hansen. 1997. Hybrid trypsinized nucleosomal arrays: identification of multiple functional roles of the H2a/H2b and H3/H4 N-termini in chromatin fiber compaction. *Biochemistry*. 36: 11381–11388.
- Van Holde, K. E. 1988. *Chromatin*. Springer, New York.
- Van Holde, K. E., and J. Zlatanova. 1996. What determines the folding of the chromatin fiber? *Proc. Natl. Acad. Sci. U.S.A.* 93:10548–10555.
- Widom, J. 1986. Physicochemical studies of the folding of the 100 Å nucleosome filament into the 300 Å filament. *J. Mol. Biol.* 190: 411–424.
- Widom, J. 1998. Structure, dynamics and function of chromatin in vitro. *Ann. Rev. Biophys. Biomol. Struct.* 27:285–327.
- Wolffe, A. P., and J. J. Hayes. 1999. Chromatin disruption and modification. *Nucleic Acids Res.* 27:711–720.
- Yao, J., P. T. Lowary, and J. Widom. 1991. Linker DNA bending induced by the core histones of chromatin. *Biochemistry*. 30:8408–8414.